# *In Situ* Fluorescence Experiments for Real-Time Monitoring of Annealed High-$T$ Latex Film Dissolution

Ö. PEKCAN,* M. CANPOLAT, and D. KAYA

Department of Physics, Istanbul Technical University, Maslak, 80626 Istanbul, Turkey

**SYNOPSIS**

A new technique, based on steady-state fluorescence measurements, is introduced for studying dissolution of polymer films. These films are formed from naphthalene and pyrene labeled poly(methyl methacrylate) (PMMA) latex particles, sterically stabilized by polyisobutylene. Diffusion of solvent (chloroform) into the annealed latex film was followed by desorption of polymer chains. Annealing was performed above $T_g$ at various temperatures for 30-min time intervals. Desorption of pyrene labeled PMMA chains was monitored in real time by the pyrene fluorescence intensity change. Desorption coefficients were found to be between 1 and $4 \times 10^{-10}$ cm$^2$/s and two different dissolution mechanisms were detected.


## INTRODUCTION

Polymer films are used for their resistance to permeation by organic solvents, water, oxygen, and other corrosive agents.[1] In that sense dissolution of polymers in organic solvents attracted attention due to the photoresist dissolution process in integrated circuits.[2-4] In controlled release applications of polymers, a solute is dispersed or molecularly dissolved in a polymer phase.[5] The release process can be controlled either by solvent diffusion or by polymer dissolution.

There are various methods to study molecular penetration in polymers. The most traditional ones are weight measurements and monitoring the redistribution of isotopic traces in the polymer.[6] The electron spin resonance (ESR) technique was used to investigate nonsolvent penetration into poly(methyl methacrylate) (PMMA) latex particles.[7] An ESR method based on the scavenging of radicals produced by high energy $\gamma$ irradiation of PMMA by oxygen was used for the measurement of the diffusion coefficient in PMMA.[8] Penetration of naphthalene molecules into PMMA latex particles stabilized by polyisobutylene (PIB) was studied by a time resolved fluorescence technique below glass transition temperature, $T_g$.[9] Fluorescence quenching and depolarization methods were used for penetration and dissolution studies in solid polymers.[10-12] An *in situ* fluorescence quenching experiment in conjunction with laser interferometry was used to investigate dissolution of PMMA film in various solvents.[4] Recently the real-time nondestructive method for monitoring small molecule diffusion in polymer films was developed.[13,14] This method is basically based on the detection of exited fluorescence molecules desorbing from a polymer film into a solution in which the film is placed.[13-16]

The penetration of organic molecules into glassy polymers often does not proceed according to the Fickian diffusion model.[17,18] Penetration not described by the Fickian model is called anomalous diffusion, where the rate of transport is entirely controlled by polymer relaxations. This transport mechanism is termed case II in contrast to Fickian diffusion, which is called case I. The dissolution of glassy polymer films can be divided into three steps. The first is the diffusion of solvent molecules into the polymer matrix. In the second step, the solvent molecules initiate the relaxation of polymer chains and a solvent-swollen gel is formed. The third and the final step consists of diffusion of polymer chains from the gel into the solvent reservoir. A schematic representation of these three sequential steps for the dissolution of glassy polymer film is shown in Figure 1. In the case II diffusion model, the second

* To whom correspondence should be addressed.

Journal of Applied Polymer Science, Vol. 60, 2105–2112 (1996)
 CCC 0021-8995/96/122105-08

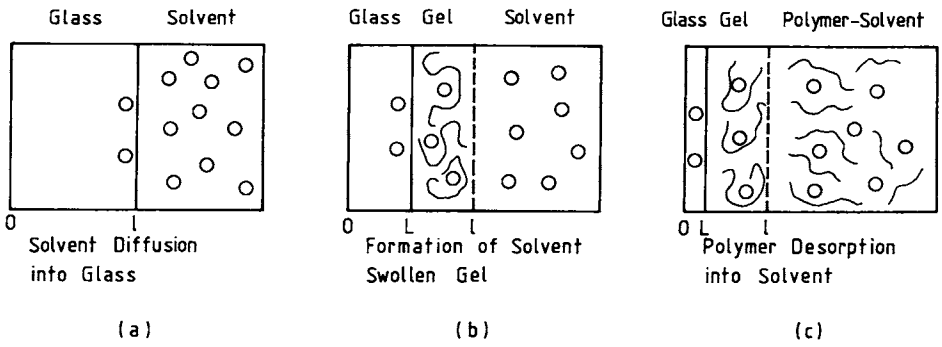


**Figure 1** Scheme of polymer film dissolution. $l$ is the film thickness and $L$ is the position of the advancing gel front.

step is the rate limiting step that predicts a linear dependence of the change in film thickness on time. The first and third steps, however, follow the case I diffusion model, where the first one is the sorption of solvent molecules by the glassy film and the third is the desorption of polymer chains from the gel layer. The polymer dissolution process can be affected by various parameters including solvent quality, polymer molecular weight, solvent thermodynamic compatibility, agitation, and temperature.

Dispersion of polymer colloid particles with glass transition temperature, $T_g$, above the drying temperature is called high-$T$ latex dispersion. These particles remain essentially discrete and undeformed during the drying process. The mechanical properties of high-$T$ powder films can be enhanced by annealing after all solvent has evaporated. This process is called sintering and is an important aspect of latex coating technology.

In this work we study the dissolution of films formed from high-$T$ latex particles labeled with pyrene (P) and naphthalene (N) dye molecules.[19] These particles have two components: the major part, PMMA, comprises 96 mol % of the material, and the minor component, PIB (4 mol %), forms an interpenetrating network through the particle interior,[20,21] which is highly soluble in certain hydrocarbons. A thin layer of PIB covers the particle surface and provides colloidal stability by steric stabilization. Film samples were prepared by annealing latex powders above $T_g$, at various temperatures for 30 min. Chloroform and heptane mixtures were used as dissolution agents. *In situ*, steady-state fluorescence (SSF) experiments were performed for real-time monitoring of the dissolution processes. The dissolution experiments were designed so that dye labeled PMMA chains desorbing from swollen gel were detected by the SSF method. Direct illumination of the film sample was avoided during the *in situ* dissolution experiment. The main goal of the presented work was to create mechanically strong films by annealing and then study the dissolution process by the novel fluorescence method.

## EXPERIMENTAL

### Material and Film Preparation

Naphthalene (N) and pyrene (P) labeled PMMA-PIB latex particles were prepared separately in a two-step process in which MMA in the first step was polymerized to low conversion in cyclohexane in the presence of PIB containing 2% isoprene units to promote grafting. The graft copolymer so produced served as a dispersant in the second stage of polymerization in which MMA was polymerized in a cyclohexane solution of the copolymer. Details were published elsewhere.[19] A stable spherical high-$T$ dispersion of polymer particles was produced, ranging in radius from 1 to 3 $\mu$m. A combination of $^1$H-NMR and UV analysis indicated that these particles contain 6 mol % PIB, 0.37 mmol N, and 0.037 mmol P groups per gram of polymer. We refer to these particles as N and P, respectively. (The particles were prepared in M. A. Winnik's Laboratory, University of Toronto, Toronto, Canada.)

To prepare the latex film the same weights of N and P particles were dispersed in heptane in a test tube. The solid contents was equal to 0.24%. Two different sets of film samples were prepared from this dispersion by placing two different numbers of drops on $3 \times 0.8$ cm$^2$ glass plates and allowing the heptane to evaporate. The liquid dispersion from the droplets covered the whole surface area of the plate andremained there until heptane evaporated. Samples were weighed before and after the film casting to determine the film thickness. The average film thicknesses were 12 and 6 $\mu$m for the first and

the second experimental sets, respectively. The average size of the particles was taken as 2 $\mu$m to estimate the number of layers or the thickness of film samples. The films were annealed in an oven for 30 min above the $T_g$ of PMMA elevating the temperature up to 210°C. The temperature was maintained within ±2°C during annealing.

For dissolution experiments two different stock solutions were prepared from mixtures of chloroform (90 and 95%) and heptane (10 and 5%). Solvents were purchased from Merck Co. (spectroscopically pure grade) and used as received. Because chloroform is a good solvent for PMMA, heptane is introduced into the mixtures to slow down the dissolution process.

### Instrumentation for Dissolution

Measurements of energy transfer during film formation and *in situ* dissolution experiments were performed using a Perkin–Elmer LS-50 spectrofluorimeter. In energy transfer measurements film samples were excited at 286-nm energy and fluorescence spectra were detected before and after annealing processes at between 300 and 480 nm. Dissolution experiments were performed in a 1.0 × 1.0 cm quartz cell equipped with a magnetic stirrer at the bottom. This cell was placed in the spectrofluorimeter and fluorescence emission was monitored at a 90° angle so that film samples were not illuminated by the excitation light. Film samples were attached at one side of a quartz cell filled with chloroform–heptane mixture. The cell was then illuminated with 345-nm excitation light. Pyrene fluorescence intensity, $I_P$, was monitored during the dissolution process at 375 nm using the "time drive" mode of the spectrofluorimeter. Emission of P-labeled polymer chains was recorded continuously at 375 nm as a function of time until there was no observable change in intensity. The dissolution cell and the film position is presented in Figure 2. Two different sets of dissolution experiments were run. In the first one, 12-$\mu$m film samples were dissolved with a (95 + 5%) chloroform–heptane mixture. In the second set a (90 + 10%) mixture was used to dissolve 6-$\mu$m film samples.

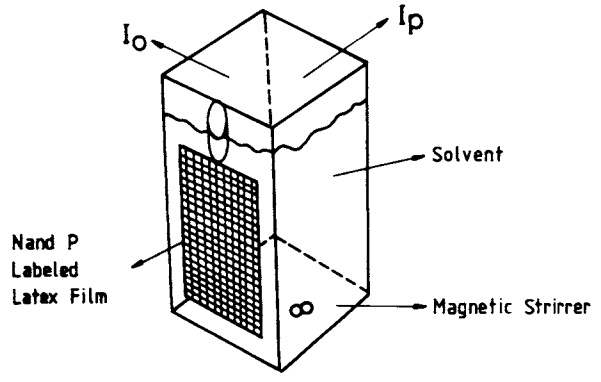


**Figure 2** Dissolution cell in LS-50 Perkin–Elmer Spectrofluorimeter. $I_0$ and $I_P$ are the excitation and emission intensities at 345 and 375 nm, respectively.

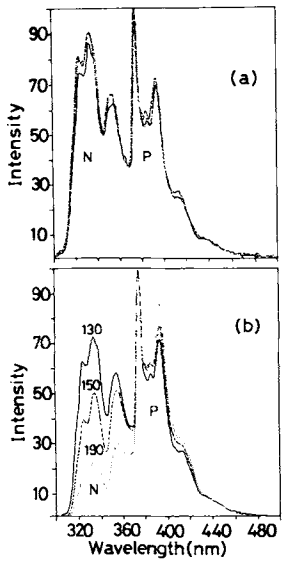


**Figure 3** Emission spectra of naphthalene (N) and pyrene (P); latex film samples are excited at 286 nm (a) before annealing and (b) after annealing for 30 min at 130, 150, and 190°C.

## RESULTS AND DISCUSSION

### Latex Film Formation

Typical fluorescence emission spectra of N–P films, excited at 286 nm, are shown in Figure 3(a,b) before and after annealing at 130, 150, and 190°C, respectively. As the annealing temperature increased, N intensity, $I_N$, decreased and P intensity, $I_P$, increased indicating that energy transfer from N to P takes place. To present the evolution of energy transfer from N to P, normalized ($I_P/I_N$) ratio was plotted as a function of annealing temperature [Fig. 4(b)]. Chloroform cast film was used to obtain normalized intensity ratios, where N–P mixing for energy transfer is almost 90%. It is seen that above 150°C energy transfer increased drastically. Direct emission intensity from pyrene ($I_{oP}$) excited at 345 nm was also plotted as a function of annealing temperature [Fig. 4(a)]. $I_{oP}$ increased, reached a maximum at 150°C, then decreased with increasing annealing temperature. This maximum in $I_{oP}$ is well under-

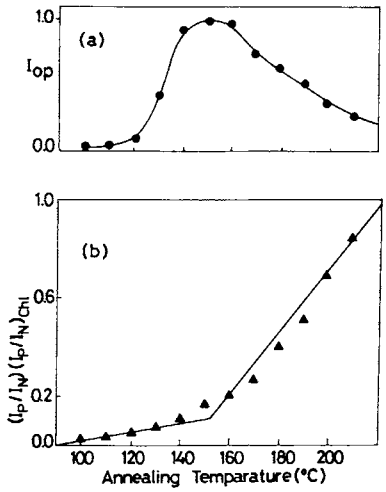


**Figure 4** (a) Variation in pyrene intensity ($I_{oP}$) with respect to annealing temperature; latex film is excited at 345 nm. (b) Plot of $(I_P/I_N)/(I_P/I_N)_{Chl}$ versus annealing temperature. $(I_P/I_N)_{Chl}$ ratio from the chloroform (Chl) cast film is used to obtain normalized intensity ratios.

stood and can be explained by the healing process at the particle–particle junction[22-25] where polymer chains relax across the junction surface. The 30-min annealing time corresponds to the healing time at 150°C. During this time the chains move at least half-way across the junction surface. Above this temperature particle boundaries start to disappear and consequently, latex film becomes mechanically strong as a result of annealing. To illustrate these findings, scanning electron micrographs of latex film annealed for 30 min at 110, 140, 160, and 210°C are presented (Fig. 5). Figure 5(a) shows high-$T$ latex particles in a powder from. In films annealed well above $T_g$, particle boundaries start to disappear as presented in Figure 5(b,c). Finally, by annealing the latex film at 210°C, one can obtain an almost transparent, mechanically strong film.

## Latex Film Dissolution

P groups labeled polymer chains were excited at 345 nm during *in situ* dissolution experiments and the variation in fluorescence emission intensity, $I_P$, was monitored with the time drive mode of the spectrofluorimeter. The chloroform–heptane mixture was well stirred so that the P labeled chains were homogeneously distributed in the fluorescence cell. P intensity, $I_P$, is plotted as a function of "dissolution time" for 12-$\mu$m film samples (Fig. 6) annealed at elevated temperatures. One can observe that as the annealing time increases, film samples start to dissolve at later times, suggesting that mechanically strong films dissolve slowly. The insert in Figure 6 shows the magnified dissolution curves at early times for samples annealed at elevated temperatures. These curves reach a plateau almost in the same fashion at long times. Dissolution curves of 6-$\mu$m film samples annealed above $T_g$ and dissolved in (90 + 10)% chloroform–heptane mixture showed similar time dependent behaviors.

## Theoretical Considerations

Various mechanisms and mathematical models were considered for the polymer dissolution. Tu and Quano[26] proposed a model that includes polymer diffusion in a liquid layer adjacent to the polymer and moving out of the liquid–polymer boundary. The key parameter for this model was the polymer disassociation rate, defined as the rate at which polymer chains desorb from the gel interface. Lee and Peppas[27] extended this model for films to express the polymer dissolution rate where gel thickness was found to be proportion to $(\text{time})^{1/2}$. A relaxation controlled model was proposed by Brochard and de Gennes[28] where after a swelling gel layer was formed, desorption of polymer from the swollen bulk was governed by the relaxation rate of the polymer stress. This rate was found to be of the same order of magnitude as the reptation time. The dependence of the radius of gyration and the reptation time on polymer molecular weight and concentration were studied, using scaling law,[29] based on the reptation model.

In this study we employed a simpler model, developed by Enscore et al.[17] to interpret the results of polymer dissolution experiments. This model includes case I and II diffusion kinetics.

## Case I or Fickian Diffusion

The solution of the 1-dimensional diffusion equation for a set of boundary conditions is sited by Crank and Park.[6] For a constant diffusion coefficient, $D$, and fixed boundary conditions, the sorption and desorption transport in and out of a thin slab is given by the following relation:

$$\frac{M_t}{M_\infty} = 1 - \frac{8}{\pi^2}\sum_{n=0}^{\infty}\frac{1}{(2n+1)^2}\exp\left(\frac{-(2n+1)^2 D\pi^2 t}{l^2}\right) \quad (1)$$

Here, $M_t$ represents the amount of materials absorbed or desorbed at time $t$, $M_\infty$ is the equilibrium amount of material, and $l$ is the thickness of the slab.

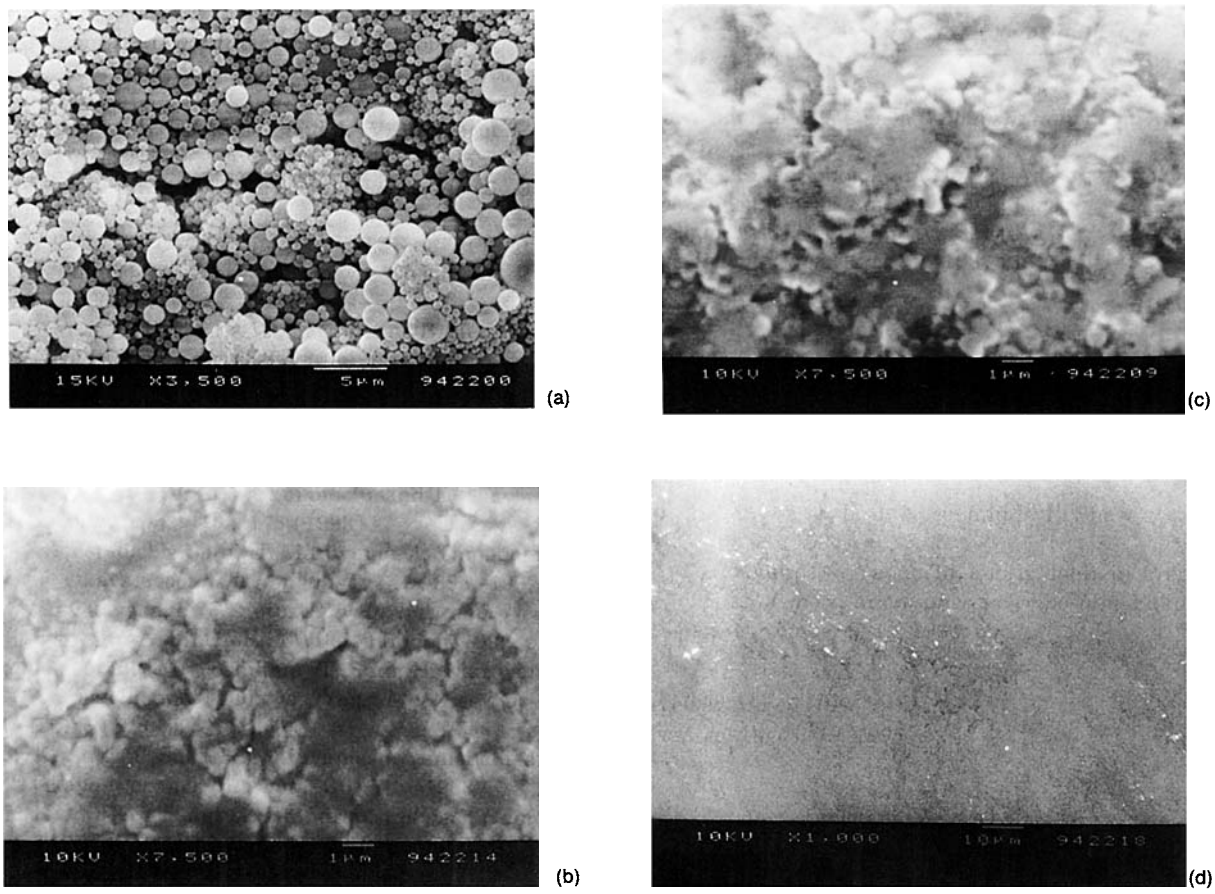


**Figure 5** Scanning electron micrographs of annealed latex film at (a) 110°C, (b) 140°C, (c) 160°C, and (d) 210°C for 30-min intervals.

## Case II Diffusion

The case II transport mechanism is characterized by the following steps. As the solvent molecules enter into the polymer film, a sharp advancing boundary forms and separates the glassy part from the swollen gel [see Fig. 1(b)]. This boundary moves into the film at a constant velocity. The swollen gel behind the advancing front is always at a uniform state of swelling. Now, consider a cross section of a film with thickness $l$, undergoing case II diffusion as in Figure 1, where $L$ is the position of the advancing sorption front, $C_0$ is the equilibrium penetrant concentration, and $k_0$ (mg/cm$^2$ min) is defined as the case II relaxation constant. The kinetic expression for the sorption in the film slab of an area $A$ is given by

$$\frac{dM_T}{dt} = k_0 A \tag{2}$$

The amount of penetrant $M_t$ absorbed in time $t$ will be

$$M_t = C_0 A(l - L) \tag{3}$$

After eq. (3) is substituted into eq. (2), the following relation is obtained:

$$\frac{dL}{dt} = -\frac{k_0}{C_0} \tag{4}$$

It can be seen that the relaxation front, positioned at $L$, moves toward the origin with a constant velocity, $k_0/C_0$. The algebraic relation for $L$ as a function of time $t$ is described by eq. (5):

$$L = l - \frac{k_0}{C_0} t \tag{5}$$

Because $M_t = Ak_0t$ and $M_\infty = C_0Al$, the following relation is obtained:

$$\frac{M_t}{M_\infty} = \frac{k_0}{C_0 l} t \tag{6}$$

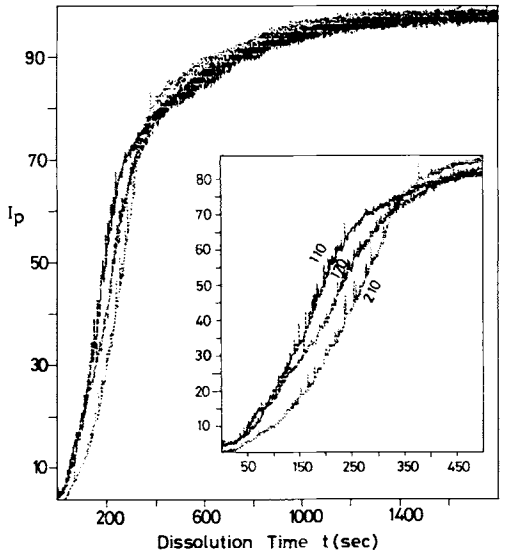


**Figure 6** Pyrene intensity, $I_P$, versus dissolution time for the film samples annealed at 110, 170, and 210°C. The cell was ilumunated at 345 nm during fluorescence measurements. Data for the plot were obtained using the time drive mode of the spectrofluorimeter. The magnified part of the plot at early time is presented in the insert.

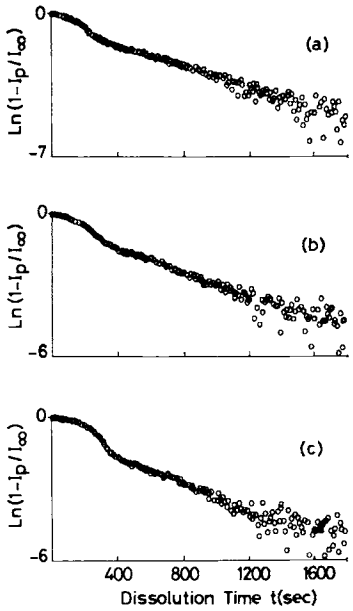


**Figure 7** Plot of the digitized data of Figure 6, which obeys the relation $\ln(1 - I_P/I_\infty) = B - At$, where $t$ is the dissolution time. (a–c) Data for samples annealed at 110, 170, and 210°C, respectively.

To quantify the dissolution curves we sought to fit the data to eq. (1). Figure 7(a–c) presents the plot of the following relation for 12-$\mu$m film samples annealed at 110, 170, and 210°C temperatures:

$$\ln(1 - I_P/I_\infty) = B - At \qquad (7)$$

This is the logarithmic form of eq. (1) for $n = 0$ with $A = D\pi^2/l^2$ and $B = \ln(8/\pi^2)$ parameters. Here, it is assumed that $I_P$ is proportional to the number of P labeled chains desorbing from the latex film and $I_\infty$ presents its value at the equilibrium condition. In Figure 7 all dissolution curves are digitized for numerical treatment. There one can observe the deviation from the linearity at early times. Similar behavior was observed for samples annealed at different temperatures and for 6-$\mu$m film samples dissolved in the chloroform–heptane mixture.

These results suggest that there are at least two different mechanisms involved during dissolution of annealed high-$T$ latex films as discussed earlier. Linear regions of the curves at long times in Figure 7 follow the Fickian diffusion model where the starting point shifts to longer times for the samples annealed at higher temperatures. When the linear portions of the curves in Figure 7 are compared to computations using eq. (7), chain desorption coefficients $D$ are obtained. The linear fit of eq. (7) to the data is presented in Figure 8(a–c). The obtained $D$ values are listed in Table I for two different sets of experiments. $D$ values for the films dissolved in 95% chloroform are found to be twice as large in magnitude as films dissolved in 90% chloroform. This is expected for the films dissolved in a higher

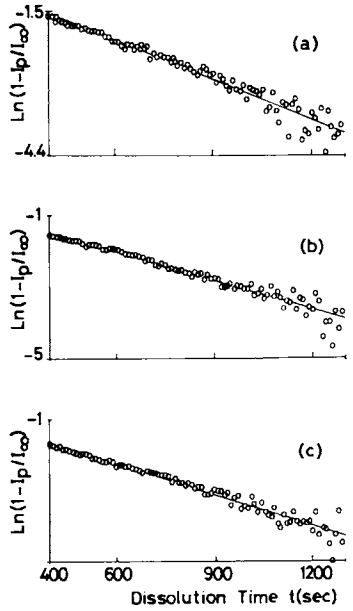


**Figure 8** Comparison of the linear portions of the data presented in Figure 7(a–c) with the computations using eq. (7). Desorption coefficients, $D$, are obtained from the slopes of the plots in (a–c) for the films annealed at 110, 170, and 210°C, respectively.

amount of good solvent. When one compares the observed $D \approx 10^{-10}$ cm$^2$/s values with the backbone diffusion coefficient of the interdiffusing polymer chains during film formation from PMMA latex particles,[30,31] ($\approx 10^{-16}$–$10^{-14}$ cm$^2$/s) 6–4 orders of magnitude difference can be seen. This is reasonable for the chains desorbing from swollen gel during dissolution of PMMA latex films. In fact, $10^{-10}$ cm$^2$/s is 2 orders of magnitude smaller than the $D$ values obtained for oxygen diffusing into PMMA spheres.[8] This may suggest that penetration of chloroform molecules into a latex film is almost as fast as desorption of PMMA chains from a swollen gel. Here one should realize that chloroform molecules are much larger in size than oxygen molecules. Our $D$ values ($10^{-10}$ cm$^2$/s) are also very close to the $D$ values ($10^{-11}$ cm$^2$/s) obtained for $n$-hexane desorption from polystyrene spheres.[17]

Short time, non-Fickian regions of the curves in Figure 7 are expanded and plotted in Figure 9(a–c) for the films annealed at 110, 170, and 210°C. $I_P/I_\infty$ plotted as a function of dissolution time; $t$ allowed quite reasonable linear fit in this region, except at very early times. If we assume that the amount of penetrant chloroform is proportional to the number of PMMA chains desorbing from the swollen gel, then eq. (6) can be written as

$$\frac{I_P}{I_\infty} = \frac{k_0}{C_0 l} t \tag{8}$$

Fitting eq. (8) to the data presented in Figure 9 yielded $k_0$ parameters. Using known $l$ and $C_0$ values, $k_0$ parameters were obtained in two sets of experiments (Table I). The $k_0$ values varied between 0.1 and 0.3 mg/cm$^2$ min. Again $k_0$ values of samples

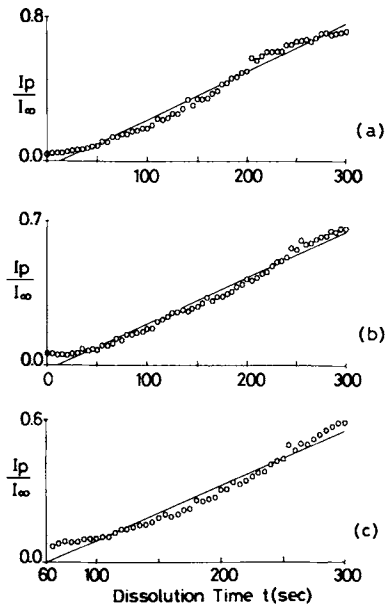


**Figure 9** Comparison of the early times region of the data presented in Figure 7(a–c) with the computations using eq. (8). Relaxation constants, $k_0$, are obtained from the slopes of the plots in (a–c) for the films annealed at 110, 170, and 210°C, respectively.

dissolved in 95% chloroform mixture were found to be twice as large as they were in the 90% mixture. This was expected due to the higher content of a good solvent. Our measurements of $k_0$ resulted in values 4 orders of magnitude different from those of Enscore et al.[17] and Jacques and Hopfenberg.[32] Thus, for $n$-heptane sorption by polystyrene spheres and film, they reported $k_0$ around $10^{-5}$ mg/cm$^2$ min. This difference can be caused by the stronger, good solvent–polymer interaction in our chloroform–PMMA system.

**Table I Results of Two Sets of Dissolution Experiments for Films Annealed at Elevated Temperatures**

| | Chloroform 90%/Heptane 10% $6 \times 10^{-4}$ cm[a] | | Chloroform 95%/Heptane 5% $12 \times 10^{-4}$ cm[a] | |
|---|---|---|---|---|
| Film Thickness $T$ (°C) | $k_0 \times 10^{-1}$ (mg/cm$^2$ min) | $D \times 10^{-10}$ (cm$^2$/s) | $k_0 \times 10^{-1}$ (mg/cm$^2$ min) | $D \times 10^{-10}$ (cm$^2$/s) |
| 110 | — | — | 2.64 | 3.48 |
| 130 | 2.08 | 0.71 | 2.26 | 4.75 |
| 150 | 1.14 | 1.29 | 2.14 | 2.13 |
| 170 | 1.14 | 1.26 | 2.23 | 3.71 |
| 190 | 1.72 | 2.02 | 2.70 | 3.06 |
| 210 | — | — | 2.93 | 3.79 |
| 230 | 1.13 | 1.02 | — | — |
| Average | 1.44 | 1.26 | 2.48 | 3.48 |

$D$ and $k_0$ values were obtained by fitting Equations 7 and 8 respectively to the data of two different sets of experiments.
[a] Film thickness.

## CONCLUSION

Dissolution process for annealed high-$T$ latex films can be separated into three stages. At a very early stage, swelling dominates and the gel layer thickness increases with time. Later, there is a period of time in which the gel thickness remains constant due to equal swelling and dissolution. Finally in the last stage, the gel thickness decreases with time due to desorption of polymer chains. In fact the first stage occurs in the first 60–100 s, depending on the annealing time of the latex film. The case II diffusion in our experiments corresponds to the time period during which gel thickness remains constant, where amounts of solvent penetration is proportional to the polymer desorption. The Fickian part of our observation range corresponds to the time region at which gel thickness decreases by rapid polymer desorption until the asymptotic value is reached. It has to be noted that the observed $D$ and $k_0$ values were found to be independent of the annealing temperature for latex film formation.

This article has introduced a novel technique for polymer dissolution monitoring that is easy to perform and inexpensive. We used simple mathematical models to produce the dissolution parameters ($D$ and $k_0$). This work will be extended to study the early stages of the dissolution process by monitoring slow gelation and to test the scaling law relations for the gel layer thickness and dissolution rate.

Ö.P. thanks Prof. M. A. Winnik for supporting his stay in Toronto last summer and supplying him with the latex material. We extend our thanks to the Turkish Academy of Sciences (TUBA) for the financial support of this work.

## REFERENCES

1. F. W. Billmeyer, Jr., *Textbook of Polymer Science,* Wiley, New York, 1984.
2. A. C. Quano, *Polym. Eng. Sci.,* **18,** 306 (1984).
3. F. Rodriguez, P. D. Krasicky, and R. J. Groele, *Solid State Technol.,* **May,** 125 (1985).
4. W. Limm, G. D. Dimnik, D. Stanton, M. A. Winnik, and B. A. Smith, *J. Appl. Polym. Sci.,* **35,** 2099 (1988).
5. P. Colombo, A. Gazzaniga, C. Caramella, U. Conte, and A. L. Manna, *Acta Pharmacol. Technol.,* **33,** 15 (1987).
6. J. Crank and G. S. Park, *Diffusion in Polymers,* Academic Press, London, 1968.
7. Z. Veksli and W. G. Miller, *J. Polym. Sci.,* **54,** 299 (1976).
8. Y. Kaptan, Ö. Pekcan, and O. Güven, *J. Appl. Polym. Sci.,* **44,** 1595 (1992).
9. Ö. Pekcan, *J. Appl. Polym. Sci.,* **49,** 151 (1993).
10. J. E. Guillet, in *Phototphysical and Photochemical Tools in Polymer Science,* M. A. Winnik, Ed., Reidel, Dordrecht, 1986.
11. T. Nivaggioli, F. Wang, and M. A. Winnik, *J. Phys. Chem.,* **96,** 7462 (1992).
12. D. Pascal, J. Duhamel, Y. Wang, M. A. Winnik, D. H. Napper, and R. Gilbert, *Polymer,* **34,** 1134 (1993).
13. L. Lu and R. G. Weiss, *Macromolecules,* **27,** 219 (1994).
14. V. V. Krongauz, W. F. Mooney, III, J. W. Palmer, and J. J. Patricia, *J. Appl. Polym. Sci.,* **56,** 1077 (1995).
15. V. V. Krongauz and R. M. Yohannan, *Polymer,* **31,** 1130 (1990).
16. Z. He, G. S. Hammond, and R. G. Weiss, *Macromolecules,* **25,** 501 (1992).
17. D. J. Enscore, H. B. Hopfenberg, and V. T. Stannett, *Polymer,* **18,** 793 (1977).
18. N. L. Thomas and A. H. Windle, *Polymer,* **23,** 529 (1982).
19. M. A. Winnik, M. H. Hua, B. Hongham, B. Williamson, and M. D. Croucher, *Macromolecules,* **17,** 262 (1984).
20. Ö. Pekcan, M. A. Winnik, and M. D. Croucher, *Phys. Rev. Lett.,* **61,** 641 (1988).
21. Ö. Pekcan, *Chem. Phys. Lett.,* **20,** 198 (1992).
22. Ö. Pekcan and M. Canpolat, *Polym. Adv. Technol.,* **5,** 479 (1994).
23. M. Canpolat and Ö. Pekcan, *Polymer,* **36,** 2025 (1995).
24. Ö. Pekcan, *Trends Polym. Sci.,* **2,** 236 (1994).
25. Ö. Pekcan, M. Canpolat, and A. Göçmen, *Polymer,* **34,** 3319 (1993).
26. Y. O. Tu and A. C. Quano, *IBM J. Res. Dev.,* **21,** 131 (1977).
27. P. I. Lee and N. A. Peppas, *J. Controlled Release,* **6,** 207 (1987).
28. F. Brochardt and P. G. de Gennes, *Phys. Chem. Hydrodynam.,* **4,** 313 (1983).
29. J. S. Papanu, D. S. Soane, and A. T. Bell, *J. Appl. Polym. Sci.,* **38,** 859 (1989).
30. M. A. Winnik, Ö. Pekcan, and M. D. Croucher, *Scientific Methods for the Study of Polymer Colloids and Their Applications,* F. Candau and R. H. Ottewill, Eds., NATO, ASI, Kluwer, New York, 1988.
31. Ö. Pekcan, M. A. Winnik, and M. D. Croucher, *Macromolecules,* **23,** 2673 (1990).
32. C. H. M. Jacques and H. B. Hopfenberg, *Polym. Eng. Sci.,* **14,** 449 (1974).

*Received May 22, 1995*
*Accepted November 5, 1995*